Linear and Nonlinear Model Predictive Control for Distributed Energy Resources in Power Grids

Gökhan Demirel[1], Xuanhao Mu[1], Tolgahan Sari[1], Giovanni De Carne[2], Kevin Förderer[1], Veit Hagenmeyer[1]
[1]Institute for Automation and Applied Informatics (IAI), Karlsruhe Institute of Technology, Germany
[2]Institute for Technical Physics (ITEP), Karlsruhe Institute of Technology, Germany
{goekhan.demirel, xuanhao.mu, tolgahan.sari, giovanni.carne, kevin.foerderer, veit.hagenmeyer}@kit.edu

***Abstract*—Modern electricity grids are increasingly integrating distributed energy resources (DERs), such as solar plants, battery storage, heat pumps, and electric vehicles. These DERs and dynamic electricity pricing introduce significant fluctuations in generation and load, necessitating advanced control strategies to maintain grid stability and economic operation. Previous research has often neglected the impact of dynamic tariffs and tended to control individual DERs separately rather than through coordinated approaches. To bridge this gap, we present eGridLVOpt, a centralized multi-objective model predictive control (MPC) framework with linear and nonlinear forms. The nonlinear MPC incorporates power flow equations as constraints to capture grid physics, increasing operational safety at the trade-off of higher computational cost. It formulates the control problem as a nonlinear program. In contrast, the linear MPC, formulated as a mixed-integer linear program, uses a simplified nodal balance power grid calculation. Both MPC variants formulate a multi-objective optimization problem balancing objectives, such as maximizing economic profit and minimizing power exchanges. Our case studies on a low-voltage distribution grid demonstrate that extending prediction horizons can increase economic gains while simultaneously reducing stress on grid components. Also, nonlinear power flow constraints are necessary to consistently maintain transformer loading within its rated capacity, ensuring safe operation without compromising profitability.**

***Index Terms*—Distributed energy resources, dynamic electricity pricing, multi-objective optimization, nonlinear model predictive control, power grid**

I. Introduction

Rudolf Emil Kálmán's pioneering work laid the foundation for many advanced control strategies, including the model predictive control (MPC). Although his work on the Kalman filter was not directly related to MPC, it provided fundamental state estimation techniques for implementing predictive control methods. Since its industrial roots in the 1970s, MPC has become a powerful tool in modern power supply systems, providing robust multi-variable control with constraint handling. It builds on optimal power flow (OPF) methods (see for instance [1] for early OPF work), which optimize generator control variables under grid constraints [2].

Modern electricity distribution grids are undergoing rapid transformation due to the growing integration of various distributed energy resources (DER), such as photovoltaic (PV) systems, battery energy storage (BES), heat pumps (HP), and electric vehicle (EV). Dynamic energy pricing schemes also significantly influence consumption patterns [3]. Although homeowners with storage-integrated PV systems benefit from lower energy costs, they may also experience higher overall consumption (rebound effect), with a recent study reporting a 7.7% increase in household energy consumption [4]. In 2023, the German Federal Ministry for Economic Affairs and Climate Action (BMWK) introduced an Electricity Storage Strategy to enhance grid resilience through load shifting with BES while simultaneously pursuing a climate-neutral energy supply by 2035 [5]. The U.S. Energy Information Administration (EIA) reports that average transmission and distribution losses remain around 5%, with up to 40% occurring in the distribution grid [6].

The dynamic nature of energy generation, prices, and exchanges require advanced control strategies, such as MPC to consider physical, safety, and operational system constraints. MPC offers a methodological framework for controlling systems in pursuit of arbitrary objectives, with applications such as peak shaving, maximizing solar self-consumption, and efficiently operating HPs. Dynamic pricing signals enable MPC to balance economic targets (e.g., cost minimization) with technical goals (e.g., peak load reduction and grid stability). Its rolling horizon optimization continuously refines control actions based on updated predictions, ensuring adaptation to changing conditions. Although several studies have applied MPC to individual components (e.g., residential batteries) and use AC power flow calculations in distribution grids, the combined influence of dynamic tariffs and the coordinated control of heterogeneous DERs remains relatively unexplored. This gap motivates the development of a centralized, multi-objective MPC framework that can address the complexities of grid operation, including high shares of intermittent PV generation, flexible loads, and volatile electricity prices.

To address these gaps, this study aims to answer the following research questions:

1) What is the combined influence of dynamic tariffs and DER heterogeneity on multi-objective MPC?
2) What trade-offs arise between linear (mixed-integer linear programming (MILP)) and nonlinear (nonlinear program (NLP)) MPC for DERs in Smart grids with respect to prediction horizon length, computational efficiency, and multiple objectives?

To answer these questions and facilitate future research, we

propose a centralized MPC framework that includes linear and nonlinear formulations. The nonlinear MPC includes detailed power flow equations as constraint formulations to capture the grid physics. This approach ensures operational safety at the cost of increased computational burden. By contrast, the linear MPC employs a simplified grid model that reduces computation time but may compromise certain stability aspects.

In this work, we extend the scope of MPC optimization to heterogeneous DERs with multi-objective goals. By managing these assets dynamically, MPC handles multi-objective goals. The main contributions of this work are:

- We present eGridLVOpt[1], an open source MPC framework implemented in NLP and MILP problem formulations. The nonlinear MPC variant is based in PYOMO [7] and uses the Interior Point OPTimizer (`IPOPT`) solver [8], while the linear MPC approach is based on Google's Operations Research Tools (OR-Tools) [9] with the PYWRAPLP interface and uses the Coin-or Branch and Cut (`CBC`) solver [10].
- We evaluate different prediction horizons (3, 6, 12, and 24 hours) under varying MPC objectives (economic cost minimization, peak shaving, and multi-objective). Our evaluation uses German electricity pricing data from EPEX Spot and ENTSO-E platforms.

This paper is structured as follows: Section II reviews state-of-the-art MPC approaches for distribution grid control. Section III presents the optimal control problem (OCP) formulation in the distribution grid, while Section IV details the modeling of the flexible DER (BES and HP) and power/pricing forecasts. Section V defines and Section VI develops the internal MPC design with different objective functions. Section VII presents and discusses the experimental settings and simulation results. Finally, Section VIII summarizes the findings and future research directions.

II. Related Work

MPC predicts a system's future behavior over a finite horizon to optimize control inputs while satisfying constraints. This process repeats with a shifted horizon at each time step, earning it the name receding horizon control (RHC). Practical application of control methods such as MPC requires multidisciplinary research [11].

We start with studies on modeling the power grid of a copper plate representation, showing that MPC with MILP improves grid operation and handles uncertainties by optimizing generator dispatch, BES, demand flexibility, and grid interaction under operational constraints [12]. For instance in [13], a probabilistic scheduling framework for renewable energy with storage using stochastic optimization and MPC to minimize power exchange between a dispatchable feeder and the grid is investigated. It models system dynamics in an aggregated and simplified way (e.g., assuming a lossless grid connection) without detailed physical equilibrium. In [14], a variable time-step formulation for large-scale DER integration is introduced, balancing computational efficiency and operational performance. Meanwhile, different MPC strategies for home microgrids with flexible thermal loads have been compared, showing that centralized coordination reduces peaks best, while hierarchically distributed approaches also reduce spikes [15]. A hierarchical-stochastic MPC framework can optimize HP, BES, and PV operations by integrating a stochastic scheduler that minimizes costs and enhances thermal comfort while handling prediction uncertainties and model inaccuracies [16].

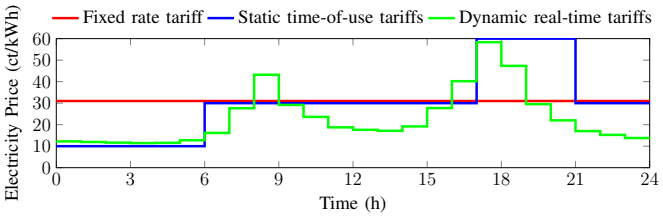

Fig. 1: Three pricing models under Germany's 2025 regulations (§14a EnWG): a fixed tariff (red), a time-of-use tariff (blue), and a dynamic tariff (green) based on hourly EPEX spot market prices on January 20, 2025.

We now focus on MPC literature integrating power flow calculations as constraints. For example, [17] proposes an MPC approach using linearized power flow constraints to regulate the active power output of a BES at a medium-voltage (MV)/low-voltage (LV) substation. Similarly, [18] introduces an MPC-based voltage regulation scheme that coordinates distributed generation, BES, and on-load tap changers (OLTCs) operations through a dual-mode strategy. The optimization of reactive power and state of charge (SoC) in preventive mode, alongside the curtailment of active power in corrective mode, stabilizes voltage rapidly in the event of severe disturbances. While [19] demonstrates the potential of MPC to reduce power exchanges and costs in the BES systems, [20] considers the impact of MPC on electrical and gas distribution grids and compares centralized and decentralized approaches to avoid grid congestion. Furthermore, [21] presents an iterative MILP approach for location-specific, cost-efficient multi-energy DERs sizing that simultaneously supports local grid-oriented services.

Many of these MPC approaches focus on scenarios with no pricing considerations or only fixed tariffs. For instance, OpenEMS [22] and EMHASS [23] each handle dynamic pricing using decentralized or device-level control. Their approaches mainly optimize local objectives, without incorporating distribution grid congestion management. However, to our best knowledge, none simultaneously incorporates full nonlinear AC power flow equations and heterogeneous DER congestion management under dynamic electricity tariffs. eGridLVOpt closes this gap by supporting both linear and nonlinear MPC to coordinate residential BES and HP. This provides DSOs and researchers with valuable insights and tools. Fig. 1 illustrates for each hour of the day three representative tariff models allowed under Germany's 2025 regulations (§14a EnWG).

[1]Code available on GitHub: https://github.com/KIT-IAI/eGridLVOpt.

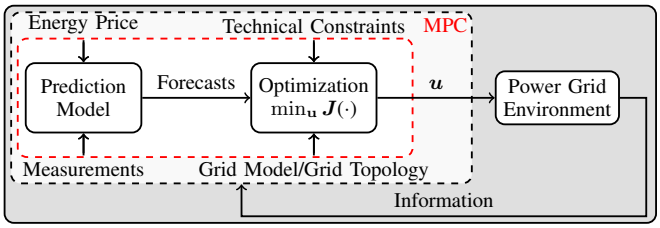

Fig. 2: Block representation of the control and environment.

III. Problem Formulation

In this paper, scalars are denoted by lowercase letters (e.g., a), while vectors are represented using bold lowercase letters (e.g., $\mathbf{a}$). Sets are indicated by calligraphic letters (e.g., $\mathcal{A}$). Subscripts are used to index DER name, nodes, time steps, or temporal horizons such as the prediction or control horizon. Specifically, i, j refers to elements in a set, where i or j denotes a single element, while discrete time steps are indexed by k. Predicted values are indicated with $\hat{a}$, and $\leq$, $\geq$ are element-wise for vectors. These notational conventions are consistently applied throughout this paper.

In this work, we adopt both linear and nonlinear MPC approaches to control the BES and HP within an electrical distribution grid. The prediction set is defined as $\mathcal{H} = \{1, 2, \ldots, n_\mathrm{p}\}$, where n_p denotes the length of the prediction time horizon. At each discrete time step $k \in \mathcal{H}$, the control actions (e.g., BES charging/discharging power or HP consumption) are denoted by $\boldsymbol{u}(k)$. The system states (e.g., bus voltages, angles, and SoC for BES) are represented by $\boldsymbol{x}(k)$. In addition, $\hat{z}(k)$ represents forecast information (e.g., demands, PV power, or electricity prices). As expressed in Eqs. (1a–1d), we aim to minimize the total cost (objective function) over the entire prediction horizon, subject to the power grid's physical laws (equality constraints), device capabilities (inequality constraints), and feasible bounds on the control variables. In mathematical form, the MPC problem for the multi-stage approach is given by:

$$\min_{\boldsymbol{u}(k)} \sum_{k=1}^{n_\mathrm{p}} J\big(\boldsymbol{x}(k), \boldsymbol{u}(k), \hat{z}(k)\big), \tag{1a}$$

subject to:

$$\boldsymbol{g}\big(\boldsymbol{x}(k), \boldsymbol{u}(k)\big) \geq 0, \tag{1b}$$

$$\boldsymbol{h}\big(\boldsymbol{x}(k), \boldsymbol{u}(k)\big) = 0, \tag{1c}$$

$$\boldsymbol{u}_\mathrm{min} \leq \boldsymbol{u}(k) \leq \boldsymbol{u}_\mathrm{max}, \qquad \forall\, k \in \mathcal{H}. \tag{1d}$$

In this framework, the function $g(\cdot)$ encapsulates the operational boundaries (e.g., line flow limits), while $h(\cdot)$ enforces the AC power flow equations. The bounds on $\boldsymbol{u}(k)$ ensure feasible setpoints for BES and HP. After applying the solution $\boldsymbol{u}(1)$ at the initial time step, the process shifts the horizon forward and repeats. The proposed MPC-based control, both linear and nonlinear, consists of several modules; the central modules are the prediction module and the optimization module, as shown in Fig. 2. The prediction module provides forecasts over multiple time horizons with solar, load, and price data. In contrast, the optimization module performs a rolling optimization considering the selected prediction settings.

IV. Controllable Grid Component Modeling

Section IV divides the modeling of flexible storage systems, loads, and building forecasts (including PV, load, and pricing data) into three parts: the BES model (IV-A), the HP model (IV-B), and the prediction of power and pricing profiles (IV-C). These controllable storage and consumption models form the fundamental basis for the internal linear and nonlinear MPC model in Section VI and its evaluation in Section VII. We consider a distribution grid with arbitrary topology as a graph $\mathcal{G} = (\mathcal{V}, \mathcal{L})$, where $\mathcal{V} = \{0, 1, \ldots, n\}$ denotes the set of buses (nodes) with $n \in \mathbb{N}^+$. Each line (edge) is defined as $l = \{i, j\}$ with $i, j \in \mathcal{V}$ and $i \neq j$, representing a connection between two nodes. The set of all lines is $\mathcal{L} = \{\{i, j\} \mid i, j \in \mathcal{V}, i \neq j\} \subseteq \mathcal{V} \times \mathcal{V}$.

A. Battery Energy Storage (BES) Modeling

The BES model is expressed in Eqs. (2a–2f), where $e_{\mathrm{BES},i}(k)$ is the energy stored in the battery at time step k, $e_{\mathrm{BES,max,i}}$ denotes the maximum energy capacity of the i-th BES, while $e_{\mathrm{BES,min,i}} = 0$ denotes its minimum; and Δk represents the time difference between the previous and the current time step. The relative self-discharge rate η_self of a BES is typically 6–7% per month [24]. In the following, we describe the BES state as well as the in- and equality constraints for all nodes $i \in \mathcal{V}_\mathrm{BES}$:

$$\begin{aligned} e_{\mathrm{BES},i}(k) = e_{\mathrm{BES},i}(k-1) &- p_{\mathrm{BES},i}(k)\,\Delta k \\ &- \eta_\mathrm{self}\, e_{\mathrm{BES,max,i}}, && \text{(2a)} \\ p_{\mathrm{BES},i}(k) = \eta_\mathrm{cha}\, p_{\mathrm{BES,cha,i}}(k) &+ \eta_\mathrm{dis}\, p_{\mathrm{BES,dis,i}}(k), && \text{(2b)} \\ 0 \leq -p_{\mathrm{BES,cha,i}}(k) &\leq p_{\mathrm{BES,cha,max,i}}, && \text{(2c)} \\ 0 \leq \quad p_{\mathrm{BES,dis,i}}(k) &\leq p_{\mathrm{BES,dis,max,i}}, && \text{(2d)} \\ e_{\mathrm{BES,min,i}} \leq e_{\mathrm{BES,i}}(k) &\leq e_{\mathrm{BES,max,i}}, && \text{(2e)} \\ p_{\mathrm{BES,cha,i}}(k)\, p_{\mathrm{BES,dis,i}}(k) = 0, & \qquad \forall k \in \mathcal{H}_p. && \text{(2f)} \end{aligned}$$

Eq. (2a) defines the energy content of the BES at any time step k. Eq. (2b) represents the control variable that controls the net power flow (charging and discharging) in the BES system at each time step k. Here, $u_{\mathrm{BES},i}(k) = p_{\mathrm{BES},i}(k)$ encapsulates the control actions on the BES, where $p_{\mathrm{BES,cha,i}}(k) \leq 0$ and $p_{\mathrm{BES,dis,i}}(k) \geq 0$ is the charging and discharging power, respectively, and η_cha, η_dis are the respective efficiencies. Eq. (2c) limits the charging power by the maximum charging power, and similarly, Eq. (2d) bounds the discharging power by the maximum discharging power. Eq. (2e) ensures physical feasibility that the energy content of the BES remains within the specified SoC limits. Lastly, Eq. (2f) guarantees that the BES cannot be charged and discharged simultaneously.

B. Heat Pump (HP) Modeling

We consider two MPC formulations for scheduling HPs. The nonlinear MPC approach, which uses continuous control variables, is formulated as a NLP. In contrast, the linear MPC approach with binary control variables and is solved as a

MILP. The 24-hour scheduling horizon is divided into four consecutive 6-hour blocks, denoted by the discrete time sets $\mathcal{H}_{6h,b}$ with $b \in \{1,2,3,4\}$. Let $p_{HP,orig,i}(k)$ denote the original (uncontrolled) power consumption profile of HP i at time step k, and $p_{HP,i}(k)$ the controlled power consumption. To limit deviations from the net heat power deviation in each 6-hour block, we introduce a tolerance parameter $\epsilon > 0$. The following equations are applied to model and operate the HPs for all nodes $i \in \mathcal{V}_{HP}$:

$$p_{HP,i}(k) \;=\; u_{HP,i}(k)\, p_{HP,max,i}, \quad \forall k \in \mathcal{H}_{6h}, \tag{3a}$$

$$\Delta p_{heat,b} \;=\; \left| \sum_{k \in \mathcal{H}_{6h,b}} \big[p_{HP,orig,i}(k) \;-\; p_{HP,i}(k)\big] \right| \;\leq\; \epsilon, \tag{3b}$$

$$u_{HP,i}(k) \;=\; \begin{cases} [0,\,1], & \text{(NLP formulation)}, \\ \{0,\,1\}, & \text{(MILP formulation)}. \end{cases} \tag{3c}$$

Eq. (3a) describes the HP power consumption $p_{HP,i}(k)$ in terms of the control variable $u_{HP,i}(k)$ and its maximum rated power $p_{HP,max,i}$. Meanwhile, Eq. (3b) ensures that, in each 6-hour block b, the total deviation of $p_{HP,i}(k)$ from its uncontrolled user demand profile $p_{HP,orig,i}(k)$ limits with the condition $\Delta p_{heat,b} \leq \epsilon$. This means there are four constraints per day, each activated within its respective block. Although the absolute value is nonlinear, the constraint Eq. (3b) can be formulated linearly by introducing auxiliary variables and separating positive and negative components. We set ϵ to half the maximum rated HP power per time step. The key difference between the nonlinear and linear formulations lies in the range of the control variable $u_{HP,i}(k)$. In the nonlinear MPC case, $u_{HP,i}(k)$ varies continuously in the intervall $[0,1]$, allowing $p_{HP,i}(k)$ to operate between 0 and $p_{HP,max,i}$. In contrast, the linear MPC follows a binary and/or integer control strategy.

C. Power and Pricing Predictions in Smart Buildings

The local power prediction for the building's Point of Common Coupling (PCC) at node $i \in \mathcal{V}$ at time $k \in \mathcal{H}$ directly follows from the predicted load $\hat{p}_{Load,i}(k) \in \mathbb{R}_{\geq 0}$ and the predicted solar generation $\hat{p}_{PV,i}(k) \in \mathbb{R}_{\geq 0}$. Depending on the chosen prediction horizon length n_p, the forecast for each building node can cover 3, 6, 12, or 24 hours and is subdivided into 15-minute intervals. In addition to the local forecast, the global forecast for the dynamic electricity price $\hat{\lambda}(k) \in \mathbb{R}$ must also be considered. Forecast noise is introduced as follows:

$$\hat{z}_{prediction}(k) = z_{orig}(k) + \xi(k), \tag{4}$$

where the predicted quantity $\hat{z}_{prediction}(k)$ representing load, PV generation, or dynamic energy price data, $\xi(k)$ represents the forecast error, modeled as Gaussian noise with zero mean and a standard deviation of 1% relative to the original value.

V. AC Power Flow Grid Constraints in MPC

Kirchhoff's laws describes the balance between generation, load flow, grid feed-in and power exchange between neighboring PCCs. The nodal power balance at node j is given by:

$$p_j + p_{PV,j} - p_{Load,j} - p_{BES,j} - p_{HP,j} = 0, \quad \forall j \in \mathcal{V}, \tag{5a}$$

$$q_j + q_{PV,j} - q_{Load,j} - q_{BES,j} - q_{HP,j} = 0, \quad \forall j \in \mathcal{V}. \tag{5b}$$

Eqs. (5a–5b) ensure active and reactive power balance at each PCC. Eqs. (6a–6b) capture active and reactive power conservation, while Eq. (6c) defines voltage drop behaviour along a distribution line derived from Ohm's law:

$$p_j + \sum_{i \in \mathcal{E}\pi(j)} \big(r_{ij}, l_{ij} - p_{ij}\big) + \sum_{k \in \mathcal{E}\sigma(j)} p_{jk} = 0, \tag{6a}$$

$$q_j + \sum_{i \in \mathcal{E}\pi(j)} \big(x_{ij}, l_{ij} - q_{ij}\big) + \sum_{k \in \mathcal{E}\sigma(j)} q_{jk} = 0, \tag{6b}$$

$$v_j^2 = v_i^2 - 2\big(r_{ij}, P_{ij} + x_{ij}, Q_{ij}\big) + \big(r_{ij}^2 + x_{ij}^2\big) l_{ij}. \tag{6c}$$

Using the standard AC power flow formulation, the active and reactive power exchange between nodes i and j is described by:

$$\begin{aligned} p_{ij}(k) = g_{ii} v_i^2(k) + v_i(k) v_j(k) \big[& g_{ij} \cos(\theta_i(k) - \theta_j(k)) \\ & + b_{ij} \sin(\theta_i(k) - \theta_j(k)) \big], \end{aligned} \tag{7a}$$

$$\begin{aligned} p_{ji}(k) = -b_{jj} v_j^2(k) + v_j(t) v_i(k) \big[& g_{ji} \sin(\theta_j(k) - \theta_i(k)) \\ & - b_{ji} \cos(\theta_j(k) - \theta_i(k)) \big], \end{aligned} \tag{7b}$$

$$\begin{aligned} q_{ij}(k) = -b_{ii} v_i^2(k) + v_i(k) v_j(k) \big[& g_{ij} \sin(\theta_i(k) - \theta_j(k)) \\ & - b_{ij} \cos(\theta_i(k) - \theta_j(k)) \big], \end{aligned} \tag{7c}$$

$$\begin{aligned} q_{ji}(k) = -b_{jj} v_j^2(k) + v_j(k) v_i(k) \big[& g_{ji} \cos(\theta_j(k) - \theta_i(k)) \\ & - b_{ji} \sin(\theta_j(k) - \theta_i(k)) \big]. \end{aligned} \tag{7d}$$

Eqs. (7a–7d) capture the active and reactive power flow in both directions, reflecting the conductance g_{ij}, susceptance b_{ij} between nodes as well as voltage angles (θ_i and θ_j). The corresponding real and imaginary current flows are:

$$\begin{aligned} \mathrm{Re}\,(i_{ij}(k)) = {} & g_{ii} v_i(k) \cos(\theta_i(k)) - b_{ii} v_i(k) \sin(\theta_i(k)) \\ & + g_{ij} v_j(k) \cos(\theta_j(k)) - b_{ij} v_j(k) \sin(\theta_j(k)), \end{aligned} \tag{8a}$$

$$\begin{aligned} \mathrm{Im}\,(i_{ij}(k)) = {} & b_{ii} v_i(k) \cos(\theta_i(k)) + g_{ii} v_i(k) \sin(\theta_i(k)) \\ & + g_{ij} v_j(k) \sin(\theta_j(k)) - b_{ij} v_j(k) \cos(\theta_j(k)), \end{aligned} \tag{8b}$$

$$\begin{aligned} \mathrm{Re}\,(i_{ji}(k)) = {} & g_{jj} v_j(k) \cos(\theta_j(k)) - b_{jj} v_j(k) \sin(\theta_j(k)) \\ & + g_{ji} v_i(k) \cos(\theta_i(k)) - b_{ji} v_i(k) \sin(\theta_i(k)), \end{aligned} \tag{8c}$$

$$\begin{aligned} \mathrm{Im}\,(i_{ji}(k)) = {} & b_{jj} v_j(k) \cos(\theta_j(k)) + g_{jj} v_j(k) \sin(\theta_j(k)) \\ & + g_{ji} v_i(k) \sin(\theta_i(k)) - b_{ji} v_i(k) \cos(\theta_i(k)). \end{aligned} \tag{8d}$$

Eqs. (8a–8d) thus detail the real and imaginary components of current flow, reflecting each branch's electrical parameters and the nodes voltage magnitudes. The technical constraints defined in Eqs. (9a–9c) ensure safe operation of the system. Specifically, node voltages remain within regulatory limits, line currents must not exceed their thermal ratings, and transformer loading should respect capacity constraints [24]:

$$v_{min} \leq v_i(k) \leq v_{max}, \tag{9a}$$

$$\sqrt{\mathrm{Re}(i_{ij}(k))^2 + \mathrm{Im}(i_{ij}(k))^2} \leq i_{ij,max}, \tag{9b}$$

$$\sqrt{p_{transformer}^2(k) + q_{transformer}^2(k)} \leq s_{transformer,max}. \tag{9c}$$

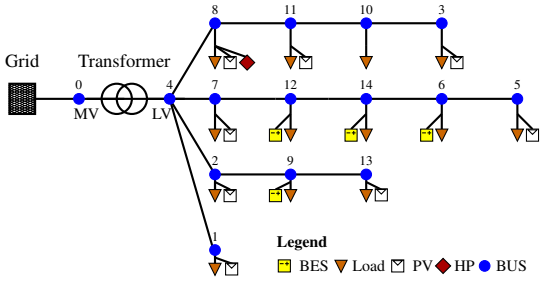

Fig. 3: 15-bus LV grid with 8 PVs, 4 BES, and 1 HP.

TABLE I: Overview of MPC controllers

Controller	Control Variable	Internal Constraints	
Linear MPC	BES Power HP Power	BES Modeling HP Modeling Nodal Power Balance	Eqs. (2a–2f) Eqs. (3a–3c) Eqs. (5a–5b)
Nonlinear MPC	BES Power HP Power	BES Modeling HP Modeling Nodal Power Balance Distribution Power Balance AC Power Flow AC Current Flow Technical Constraints	Eqs. (2a–2f) Eqs. (3a–3c) Eqs. (5a–5b) Eqs. (6a–6c) Eqs. (7a–7d) Eqs. (8a–8d) Eqs. (9a–9c)

VI. Linear and Nonlinear MPC Objectives

We formulate a centralized optimization problem for the dynamic operation of the BES and HP, relying on both linear and nonlinear MPC controllers. Table I summarizes control variables and constraints for linear and nonlinear MPC formulations. The MPC objectives are as follows:

1) Economic objective (minimizes electricity costs):

$$J_1 = \sum_{k=1}^{n_\mathrm{p}} \sum_{j \in \mathcal{V}} \lambda(k) \left(p_{\mathrm{import},j}(k) + p_{\mathrm{export},j}(k) \right) \tag{10}$$

where $p_{\mathrm{import},j}$ and $p_{\mathrm{export},j}$ represent buying and selling power, respectively, and $\lambda(k)$ is the dynamic price.

2) Grid-oriented objective (minimizes power exchanges):

$$J_2 = \begin{cases} \sum_{k=1}^{n_\mathrm{p}} \sum_{j \in \mathcal{V}} (p_j)^2, & \text{(NLP formulation)} \\ \sum_{k=1}^{n_\mathrm{p}} \sum_{j \in \mathcal{V}} |p_j|, & \text{(MILP formulation)} \end{cases} \tag{11}$$

where penalizing $(p_j)^2$ or $|p_j|$ curbs large power peaks to maintain a near-constant baseline demand.

3) Multi-objectives (economic and power exchange):

$$\min_{\mathbf{u}} J = \min_{\mathbf{u}} (\omega \cdot f(J_1) + (1-\omega) \cdot f(J_2)) \;\forall\; \omega \in [0,1] \tag{12}$$

where ω weights the relative importance of power exchange versus cost minimization. The function $f(\cdot)$ applies a z-score normalization by subtracting the mean and dividing by the standard deviation of the objective values. This ensures that both objectives remain on a comparable scale. Nonlinear MPC is formulated as an NLP due to its nonlinear constraints and an objective function that combines a linear economic term with a quadratic power exchange term. In contrast, linear MPC, solved as a MILP, employs a piecewise linear economic objective and an absolute-value-based power exchange objective, maintaining only linear constraints.

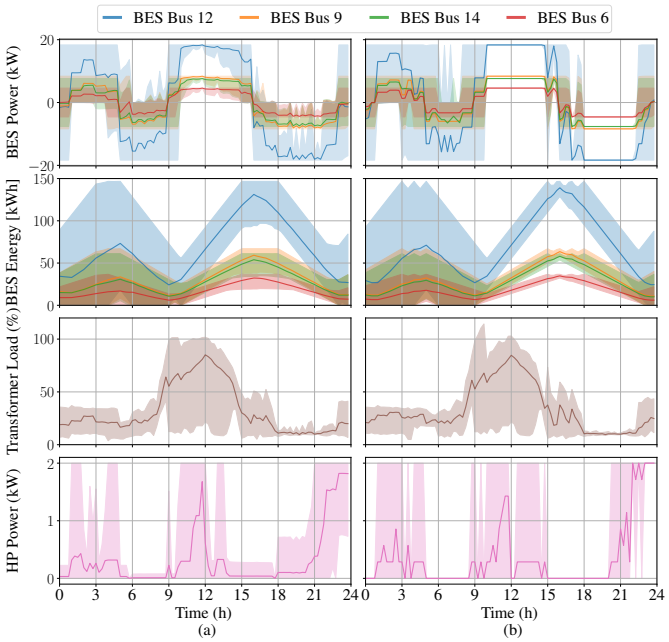

Fig. 4: Comparison of nonlinear (a) and linear (b) MPC under equal weighting, showing average BES power (kW), BES energy capacity (kWh), transformer load (%), and HP power (kW) over seven days, representation as a single averaged day with shaded regions indicating min and max values.

VII. Results

This section presents the simulation setup (VII-A) and compares the BES's charging and discharging behavior, the SoC in kWh (representing BES energy capacity), and transformer loading for the proposed linear and nonlinear MPC approaches (VII-B). Additionally, a sensitivity analysis is conducted for linear MPC and nonlinear MPC with and without a fixed transformer constraint (VII-C).

A. Simulation Setup

This section describes the experimental settings and evaluates the proposed linear and nonlinear MPC approaches across various experiments. Fig. 3 illustrates the 15-bus distribution grid topology used for validation, including installed DER systems. Load and PV profiles for validation are from Simbench [25]. We consider representative metrics such as BES charging/discharging power, SoC, transformer loading [24], economic profit, and power exchange. Additionally, we investigate the influence of prediction horizons n_p (3h, 6h, 12h, and 24h) and objective weighting. The weighting parameter ω defined in Eq. (12) ranges from 0.0 to 1.0 in increments of 0.1, enabling a systematic analysis of trade-offs between power exchange and cost minimization. We use historical EPEX spot market prices (March 20–27, 2024) to capture real-world dynamic tariff variations, highlighting the impact of dynamic pricing on MPC performance.

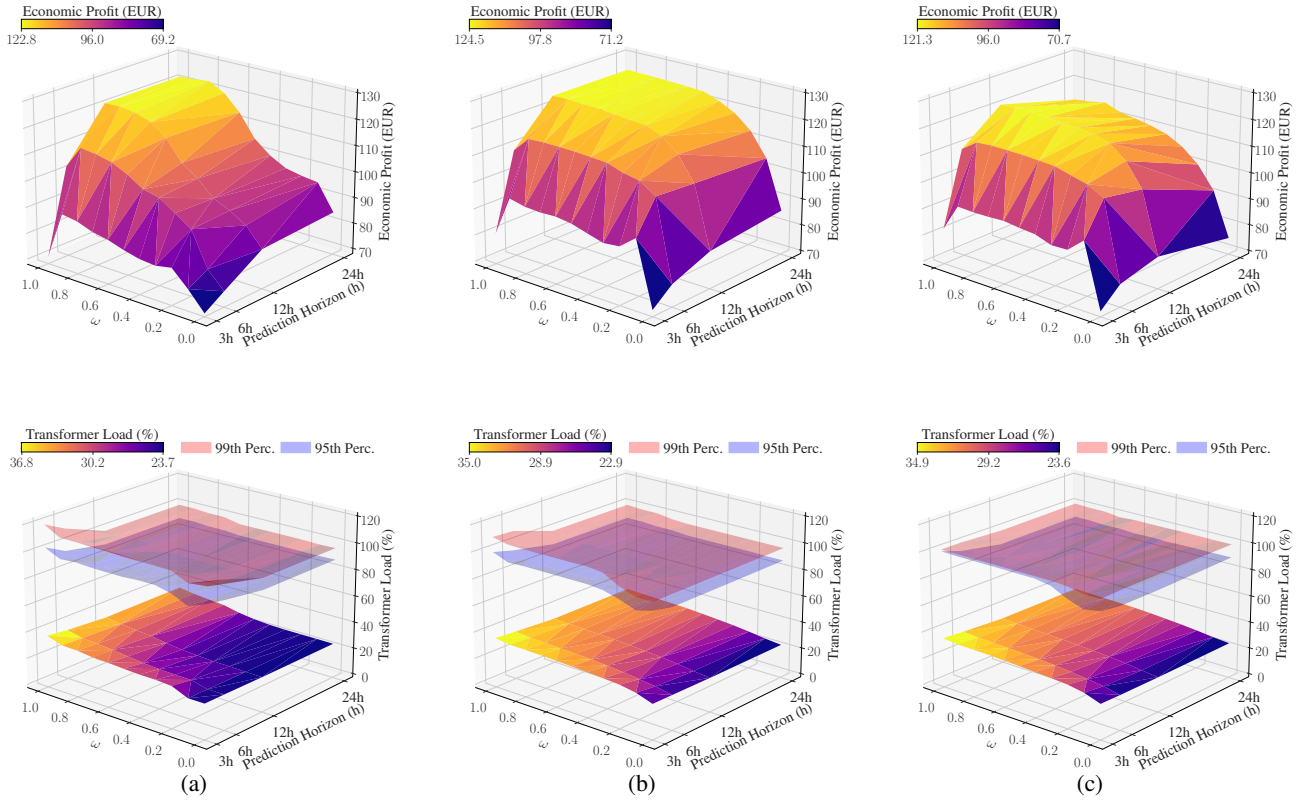

Fig. 5: Sensitivity analysis under varying weightings and prediction horizons (3h, 6h, 12h, 24h) for a one-week simulation. Top: Economic profit (EUR); Bottom: Transformer load (%). Subfigures: (a) linear MPC, (b) nonlinear MPC, (c) nonlinear MPC with transformer load constraint.

B. Baseline Analysis with fixed Horizon and Weighting

First, we perform a baseline scenario analysis comparing linear MPC without and nonlinear MPC with maximum transformer constraint allowing up to 100% of its rated apparent power. We use a 24-hour prediction horizon and equal objective weighting as defined in Eq. (12). This scenario provides baseline insights into BES charging/discharging behavior, SoC trajectories, transformer loading, and HP power consumption. Fig.4 illustrates these metrics over a one-week simulation period. Maximum BES capacities vary by location: 146.7kWh at Bus12, 67.0kWh at Bus9, 61.1kWh at Bus14, and 36.7kWh at Bus6 (see Fig. 3). Nonlinear MPC yields smoother charging and discharging trajectories compared to linear MPC, which exhibits abrupt changes (see Fig. 4a). Conversely, Fig. 4b shows that linear MPC demonstrates more flexibility under dynamic pricing by not enforcing nonlinear constraints required for physical equilibrium. In contrast, nonlinear MPC employs a conservative control strategy to comply with the fixed transformer constraint, shifting peak power flows to periods of lower energy flow (e.g., 18:00–21:00). A similar pattern occurs for HP control. Linear MPC reduces HP operation during high price periods (e.g., 15–21h), while nonlinear MPC leverages these intervals to shift peak power flows and satisfy transformer constraints.

TABLE II: Simulation Runtime Analysis for MPC.

Prediction Horizon	**Linear MPC (s)**	**Nonlinear MPC (s)**	
		I	***I****
3h	$39 \pm 6s$	$673 \pm 32s$	$937 \pm 40s$
6h	$46 \pm 5s$	$1299 \pm 46s$	$1893 \pm 52s$
12h	$60 \pm 5s$	$2793 \pm 118s$	$4347 \pm 132s$
24h	$91 \pm 11s$	$6278 \pm 580s$	$10365 \pm 466s$

I^* with a transformer constraint $s_{\text{transformer,max}} = 100\%$ in Eq. (9c).

C. Sensitivity Analysis with Varying Horizon and Weighting

This sensitivity analysis evaluates the influence of different prediction horizons and the objective weighting on the linear and nonlinear MPC with and without the transformer loading constraint. The x-axis denotes the weighting parameter ω, the y-axis the prediction horizons, and the z-axis the associated metrics (economic or transformer load). Here, $\omega = 1$ indicates a fully economic objective to maximize profitability, while $\omega = 0$ indicates grid-supportive operation by minimizing power exchanges. Fig. 5a shows the linear MPC that the transformer load increases with increasing economic weight. Despite the higher economic weight $\omega = 1$, the profitability performance is worse than with a lower weighting. The narrow three-hour prediction horizon restricts optimal control actions under dynamic tariffs, resulting in suboptimal solutions and motivating alternative short-horizon decision-making methods.

Short horizons yield suboptimal control due to limited foresight, motivating alternative approaches. However, the solution tends towards a more optimal economic performance as the prediction horizon increases. On the other hand, fully grid-oriented operation $\omega = 0$ leads to the lowest transformer load rates. With an increasing prediction horizon, economic performance also increases. Fig. 5b demonstrates that the nonlinear MPC is more profitable and grid-friendly than the linear MPC. Integrating AC power flow constraints and economic goals within nonlinear MPC reduces transformer loading. Increasing the prediction horizon can reduce maximum transformer loading to less than 100% without negatively impacting profitability. As shown in Fig. 5c, the behavior of the nonlinear MPC with transformer constraints is very similar to that of nonlinear MPC without constraints. Consequently, transformer loading is strictly limited to its rated apparent power (100% loading). For short horizons with $\omega = 0.0$, the transformer load remains minimal at the 95th percentile but increases as ω grows closer to 1.0. This additional fixed transformer constraint in nonlinear MPC causes economic penalties, decreasing the maximum, average, and minimum profits by around 2.57%, 1.84%, and 0.70%, respectively. Compliance with the 100% transformer limitation distributes the power flow over a longer period, slightly increasing the average transformer load. Consequently, average transformer overload decreases from 36.8% (linear MPC) and 35.0% (unconstrained nonlinear MPC) to 34.9%. Table II presents the mean and standard deviation of computational time (in seconds) for a one-week sensitivity analysis simulation. Nonlinear MPC with the transformer constraint requires significantly more computation than MPC without the transformer constraint. Specifically, for a three-hour prediction horizon, the computation time increases by about 39%, while for a 24-hour horizon, this difference increases to about 65%. Therefore, applying transformer constraints in nonlinear MPC adds a computational burden.

VIII. Conclusion and Outlook

In this paper, we use our eGridLVOpt implementation (available on GitHub at https://github.com/KIT-IAI/eGridLVOpt) to conduct a series of experiments comparing linear and nonlinear MPC approaches for coordinating heterogeneous DERs. We carefully consider solver selection, handling conflicting multi-objective trade-offs, and computational budgets to ensure a fair comparison. Our evaluation campaign provides quantitative insights into representative scenarios and clarifies key decision criteria for choosing between linear and nonlinear MPC. In summary, these results highlight: (i) the efficiency of nonlinear formulations in achieving peak-load reduction, (ii) the economic and grid-oriented advantages of longer prediction horizons, and (iii) the need for alternative methods at shorter horizons to avoid suboptimal decision-making.

Future research could focus on integrating electric vehicles or high grid penetration scenarios involving additional energy storage systems and heat pumps. Another promising direction is leveraging Inverse Reinforcement Learning with this MPC expert data to control the distribution grid components.

IX. Acknowledgements

This work was supported in part by the Energy System Design (ESD) Project; in part by the Helmholtz Association's Initiative and Networking Fund through Helmholtz AI; and the HAICORE@KIT partition.

References

[1] H. W. Dommel and W. F. Tinney, "Optimal Power Flow Solutions," *IEEE Trans. Power App. Syst.*, vol. PAS-87, pp. 1866–1876, 1968.
[2] C. E. García *et al.*, "Model predictive control: Theory and practice–A survey," *Automatica*, vol. 25, no. 3, pp. 335–348, 1989.
[3] J. Stute and M. Kühnbach, "Dynamic pricing and the flexible consumer – Investigating grid and financial implications: A case study for Germany," *Energy Strategy Reviews*, vol. 45, p. 100987, 2023.
[4] E. Aydın *et al.*, "The rebound effect of solar panel adoption: Evidence from Dutch households," *Energy Economics*, vol. 120, p. 106645, 2023.
[5] Federal Ministry for Economic Affairs and Climate Action (BMWK), "Electricity Storage Strategy," Berlin, Germany, Dec. 2023.
[6] U.S. Energy Information Administration, "Frequently Asked Questions (FAQs)," https://www.eia.gov, Nov. 2023.
[7] M. L. Bynum *et al.*, *Pyomo – Optimization Modeling in Python*, 3rd ed., ser. Springer Optim. Appl. Springer Cham, 2021, vol. 67.
[8] A. Wächter and L. T. Biegler, "On the implementation of an interior-point filter line-search algorithm for large-scale nonlinear programming," *Mathematical Programming*, vol. 106, no. 1, pp. 25–57, Mar 2006.
[9] L. Perron and V. Furnon, "OR-Tools," Google, May 2024, software. [Online]. Available: https://developers.google.com/optimization/
[10] J. Forrest *et al.*, "coin-or/Cbc: Release 2.10.12," Aug. 2024, software. [Online]. Available: https://doi.org/10.5281/zenodo.13347261
[11] J. Drgoňa *et al.*, "All you need to know about model predictive control for buildings," *Annual Reviews in Control*, vol. 50, pp. 190–232, 2020.
[12] A. Parisio *et al.*, "A Model Predictive Control Approach to Microgrid Operation Optimization," *IEEE Trans. Control Syst. Technol.*, vol. 22, no. 5, pp. 1813–1827, 2014.
[13] R. R. Appino *et al.*, "On the use of probabilistic forecasts in scheduling of renewable energy sources coupled to storages," *Applied Energy*, vol. 210, pp. 1207–1218, 2018.
[14] A. T. Eseye *et al.*, "Scalable Predictive Control and Optimization for Grid Integration of Large-scale Distributed Energy Resources," in *2022 IEEE PESGM*, Denver, CO, USA, 2022, pp. 01–05.
[15] D. I. Hidalgo-Rodríguez and J. Myrzik, "Optimal Operation of Interconnected Home-Microgrids with Flexible Thermal Loads: A Comparison of Decentralized, Centralized, and Hierarchical-distributed Model Predictive Control," in *2018 PSCC*, Dublin, Ireland, 2018, pp. 1–7.
[16] F. Langner *et al.*, "Hierarchical-stochastic model predictive control for a grid-interactive multi-zone residential building with distributed energy resources," *J. Build. Eng.*, vol. 89, p. 109401, 2024.
[17] A. Giuseppi *et al.*, "Model Predictive Control of Energy Storage Systems for Power Regulation in Electricity Distribution Networks," in *Proc. IEEE SMC, 2019*, 2019, pp. 3365–3370.
[18] Y. Guo *et al.*, "MPC-Based Coordinated Voltage Regulation for Distribution Networks With Distributed Generation and Energy Storage System," *IEEE Trans. Sustain. Energy*, vol. 10, no. 4, pp. 1731–1739, 2019.
[19] F. Mueller *et al.*, "Energy Optimization Controllers for Residential Peak Load Shaving and Cost Minimization," in *Proc. ISGT Europe*, 2023, pp. 1–6.
[20] F. Mueller, S. de Jongh *et al.*, "Sector-Coupled Distribution Grid Analysis for Centralized and Decentralized Energy Optimization," in *2023 58th UPEC*, 2023, pp. 1–6.
[21] S. Grafenhorst *et al.*, "Grid Aware Portfolio Optimization of a Multi-Energy DER," in *2024 iSPEC*, 2024, pp. 245–250.
[22] S. Feilmeier *et al.*, "Openems/openems: 2025.3.0," Mar. 2025. [Online]. Available: https://doi.org/10.5281/zenodo.14952378
[23] D. Hernandez *et al.*, "EMHASS – energy management for home assistant," https://github.com/davidusb-geek/emhass, 2025.
[24] G. Demirel *et al.*, "PIDE: Photovoltaic Integration Dynamics and Efficiency for Autonomous Control on Power Distribution Grids," *Energy Informatics*, vol. 8, no. 1, p. 32, March 2025.
[25] C. Spalthoff *et al.*, "SimBench: Open Source Time Series of Power Load, Storage, and Generation for Simulation of Electrical Distribution Grids," in *Proc. Int. ETG-Congr.; ETG Symp.*, 2019, pp. 1–6.